J. Biochem. **133**, 279–286 (2003)
DOI: 10.1093/jb/mvg038

Glu-53 of *Bacillus cereus* Sphingomyelinase Acts as an Indispensable Ligand of Mg^{2+} Essential for Catalytic Activity

Takashi Obama, Yukie Kan, Hiroh Ikezawa, Masayoshi Imagawa and Kikuo Tsukamoto*

Department of Molecular Biology, Graduate School of Pharmaceutical Sciences, Nagoya City University, 3-1 Tanabe-dori, Mizuho-ku, Nagoya, Aichi 467-8603

Received October 31, 2002; accepted December 18, 2002

Bacillus cereus **sphingomyelinase (SMase) is an extracellular hemolysin classified into a group of Mg^{2+}-dependent neutral SMases (nSMase). Sequence comparison of bacterial and eukaryotic Mg^{2+}-dependent nSMases has shown that several amino acid residues, including Glu-53 of *B. cereus* SMase, are conserved, suggesting a catalytic mechanism common to these enzymes. Mutational analysis has revealed that hemolytic and SM-hydrolyzing activities are abolished by E53A and E53Q mutations. Only the E53D mutant enzyme partially retains these activities, however, a significant decrease in the apparent k_{cat}/K_m for SM hydrolysis is observed by this mutation. Mg^{2+} activates the wild-type enzyme in a two-step manner, *i.e.*, at least two binding sites for Mg^{2+}, high- and low-affinity, are present on the enzyme. The binding affinity of essential Mg^{2+} for the high-affinity site is decreased by the mutation. In addition, the binding affinities of Mn^{2+} and Co^{2+} (substitutes for Mg^{2+}) are also decreased. On the contrary, the inhibitory effects of Ca^{2+}, Cu^{2+}, and Zn^{2+} on SM-hydrolyzing activity are not influenced by the mutation. The results indicate that Glu-53 of *B. cereus* SMase acts as a ligand for Mg^{2+} and is involved in the high-affinity Mg^{2+}-binding site, which is independent of the binding site for inhibitory metals.**

Key words: active site, cation-binding, hemolysis, phospholipase C, sphingomyelin.

Abbreviations: aSMase, acidic sphingomyelinase; bSMase, basic sphingomyelinase; EXOIII, exonuclease III; HAP1, human apurinic/apyrimidinic endonuclease 1; HNP, 2-hexadecanoylamino-4-nitrophenylphosphocholine; Lyso-PC, lysophosphatidylcholine; nSMase, neutral sphingomyelinase; *p*-NPPC, *p*-nitrophenylphosphocholine; SM, sphingomyelin; SMase, sphingomyelinase; WT, wild type.

Sphingomyelinase (SMase, sphingomyelin phosphodiesterase; EC 3.1.4.12), which catalyses the hydrolysis of sphingomyelin (SM) to phosphocholine and ceramide, is widely distributed from bacteria to primates. All SMases are classified by their optimal pH, cation requirement and localization as acidic SMase (aSMase), Zn^{2+}-dependent aSMase (*1*), neutral SMase (nSMase) (*2*), Mg^{2+}-dependent nSMase (*3*, *4*) ,or basic SMase (bSMase) (*5*). *Bacillus cereus* SMase is one of a group of bacterial extracellular toxins, and exhibits potent hemolytic activity against SM-rich erythrocytes in mammals such as ruminants (*6*). The enzyme is a member of the Mg^{2+}-dependent nSMases, and is activated by Mn^{2+} and Co^{2+} as well as Mg^{2+}, but inhibited by Ca^{2+}, Cu^{2+}, Zn^{2+}, and EDTA (*7*). The enzyme acts on SM-rich erythrocyte membranes, selectively hydrolyses SM, and then brings about physiological instability of the membrane. After the hydrolysis of SM, so-called "hot-cold hemolysis" occurs when the reaction mixture is cooled to 4°C due to phase transition of the lipid bilayer of the membrane. Also, *Staphylococcus aureus* β-toxin, a Mg^{2+}-dependent nSMase, shows representative hot-cold hemolysis. In addition to the hot-cold lysis, *B. cereus* SMase induces "hot lysis" without cooling due to exhaustive hydrolysis of SM on the outer leaflet of the erythrocyte membrane (*6*, *8*).

In eukaryotic cells, the SMase that exhibits its optimal activity at neutral pH (nSMase), has been extensively investigated over the past decade, because the enzyme plays a role as one of the key enzymes in sphingolipid metabolism in mammalian cells. Ceramide and sphingosine 1-phosphate, derived from SM metabolism, are involved in many cellular events such as signal transduction, proliferation, differentiation and apoptosis (*9*, *10*). Recently, two independent cDNAs of membrane-binding Mg^{2+}-dependent nSMases, nSMase 1 (*3*) and nSMase 2 (*4*), were cloned. These eukaryotic nSMases are present in a membrane-associated form due to their hydrophobic stretch. Sequence comparison of both nSMases with bacterial SMases revealed that several amino acid residues that are conserved in the bacterial enzymes are also conserved in the eukaryotic ones, indicating that these residues are important for enzymatic function. For instance, His-151 and His-296, essential residues in *B. cereus* SMase for catalysis (*11*), are also conserved in eukaryotic nSMase, suggesting that basic research on SMase of *B. cereus* not only provides information on the mechanism of toxin action, but also can be applied to research on sphingolipid metabolism in mammalian cells.

We previously estimated the 3D structural model of *B. cereus* SMase based on its 3D-1D structural compatibility

*To whom correspondence should be addressed. Tel: +81-52-836-3458, Fax: +81-52-836-3457, E-mail: kikuot@phar.nagoya-cu.ac.jp


```
Bovine DNase I     29-VRRYDIVLIQEVRDSHLVAVGKLLDYLNQDD- 59

B.cereus           43-IKNQDVVILNEVFDN--SASDRLLGNLKKEY- 71
L.interrogans      94-IQNQDVIVFDEAFDT--DARKILLDGVRSEY-122
S.aureus           42-IKNNDVVIFNEAFDN--GASDKLLSNVKKEY- 70
human (nSMase1)    39-QESFDLALLEEVYSE--QDFQYLRQKLSPTY- 67
human (nSMase2)   354-PANLDFLCLQEVFDK--RAATKLKEQLHGYF-382
```

Fig. 1. **Partial alignment of bovine pancreatic DNase I and the Mg^{2+}-dependent nSMases from *B. cereus*, *Leptospira interrogans*, and *S. aureus* (*12*), with human nSMase 1 (*3*) and human nSMase 2 (*4*).** The numbering indicates the mature sequences of the secretory bacterial enzymes and complete ORFs of the eukaryotic enzymes. The conserved Glu residues among these SMases are boxed.

with that of bovine pancreatic DNase I (*12*). These two enzymes are members of a phosphodiesterase superfamily. The model shows that Glu-53 is located beside the two catalytic histidine residues, His-151 and His-296, in the active site cleft. Furthermore, alignment of the primary sequences of bacterial and human Mg^{2+}-dependent nSMases shows that Glu-53 is conserved among all the enzymes (Fig. 1). These data strongly suggest that Glu-53 may be responsible for the catalytic function of the enzyme. In this study, we investigated the functional role of Glu-53 as a metal ligand in the enzymatic action of *B. cereus* SMase.

MATERIALS AND METHODS

Enzyme Substrates—As the substrate for the SMase assay, SM was prepared as follows (*13*). Total crude lipid was extracted from bovine brain by the method of Bligh and Dyer (*14*). Glycerolipids, glycerophospholipids and glycolipids were degraded by acid and alkaline methanolysis, and the sphingolipid fraction was obtained by acetone precipitation. From the resulting precipitate, SM was purified by silicic acid column chromatography. The purified SM comprised two molecular species composed of 16:0- and 24:1-ceramide backbones by mass spectrometrical analysis (data not shown). Other phosphocholine-containing substrates, HNP, Lyso-PC, and *p*-NPPC, were purchased from Sigma.

Construction of the Mutant SMase—The plasmid pUCSM2, carrying the *B. cereus* SMase gene (*15*) in pUC119, was used as a template for PCR-mediated site-directed mutagenesis (*16*). Forward and reverse oligonucleotide primer pairs containing the intended specific mutations were prepared for the mutagenesis. The PCR product was treated with *Dpn* I to digest template plasmid DNA for 1 h, and then transformed into *Escherichia coli* strain TG1. Every mutant gene was sequenced to prove it to have only the desired mutation.

Preparation of Crude Cell Extract—E. coli harbouring the WT or mutant SMase gene were cultured in 2× YT medium. At late logarithmic growth phase, cultured cells were collected by centrifugation at 500 ×*g*, washed with physiological saline (0.145 M NaCl) at room temperature, resuspended in ice-cold 40 mM Na borate buffer (pH 7.5) and then disrupted by sonication. After centrifugation at 100,000 ×*g* for 10 min at 4°C, the supernatant was recovered and used as a crude enzyme source.

Purification of WT and Mutant SMases—Mass production of WT and mutated SMases was performed by the method reported previously (*17*). Mutated SMase genes were excised by *Bsp*HI and *Xba*I digestion, inserted into $pNU211r_2l_5$ and then introduced into *Bacillus brevis* 47. Purification of SMase from the culture medium of the *B. brevis* transformant was also performed by the method previously reported (*11*). Briefly, the enzyme activity was precipitated with 80% saturated $(NH_4)_2SO_4$ from the culture medium, and fractionated by DEAE-ion exchange chromatography. The active fraction was thoroughly separated by gel filtration chromatography. The purity of the final preparation was confirmed by SDS–PAGE.

Assay of Enzyme Activity: Hemolytic Activity—A handy system to evaluate the hemolytic activity of mutant SMases was developed as follows. *E. coli* TG1 strains harbouring mutant SMase genes were streaked on YT agar plates containing 2.5% bovine erythrocytes, cultured for 16 h at 37°C, and then left to stand at 4°C until hemolytic zones became clear. The hemolytic activity of the purified enzyme was determined by incubating the enzyme protein with 2.5% bovine erythrocytes in 40 mM Na borate buffer (pH 7.5)/4 mM $MgCl_2$/0.02% BSA/0.75% NaCl at 37°C for 30 min, followed by centrifugation at 500 ×*g*. The percentage of hemolysis was evaluated by A_{550} of the supernatant of the reaction mixture.

Assay of Enzyme Activity: Hydrolytic Activity—The hydrolytic activity of WT and mutant SMases were measured using SM, HNP, *p*-NPPC (*18*), and lyso-PC (*11*) as substrates according to the method previously reported. One unit of enzyme activity was defined as the activity that hydrolyzed 1 μmol of substrate per min at 37°C for all substrates.

Each experiment was performed at least three times and all hemolytic and hydrolytic activities are expressed as mean values with SD.

Measurement of the Amount of Divalent Cation Bound to SMase—Enzyme solution (10 μM) in 10 mM Tris-HCl (pH 7.5) was incubated at 37°C with excess amount of divalent cation for 30 min, and then free cations were removed by ultrafiltration. Thereafter, the protein amount was quantified by absorbance at 280 nm using a molar extinction coefficient of 58,200 $M^{-1}\cdot cm^{-1}$, and the amount of divalent cations bound to the enzyme was determined using a Shimadzu Atomic Absorption/Flame spectrophotometer AA-660. All data are expressed as mean values with SD and are from at least three independent experiments.

RESULTS

Effect of Glu-53 Mutation on SMase Activity—In the 3D model of *B. cereus* SMase, Glu-53 is located in the vicinity of catalytic residue His-151, suggesting that Glu-53 is important for the catalytic function of the enzyme. To investigate the role of Glu-53 in the catalytic site of SMase, this residue was replaced with Ala, Gln or Asp by site-directed mutagenesis using pUCSM2, the WT plasmid clone of *B. cereus* SMase gene, as a template. After confirmation of the entire sequences of the PCR

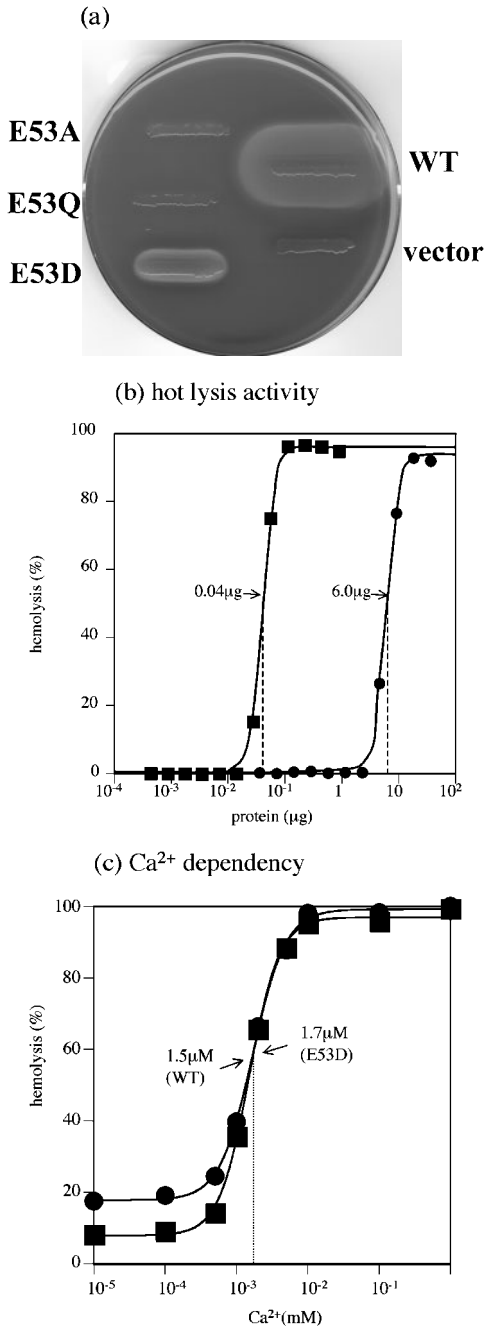

Fig. 2. **Effect of Glu-53 substitution on hemolytic activity.** (a) *E. coli* TG1 cells expressing the WT or Glu-53-mutated SMase protein, were incubated on a YT agar plate containing 2.5% bovine erythrocytes at 37°C for 16 h, and then chilled at 4°C until the hemolytic zones became clear. Hemolytic activities of the SMases were evaluated by the area size of the hemolytic zones. (b) The WT (solid square) and E53D (solid circle) mutant enzymes were incubated with a 2.5% aqueous suspension of bovine erythrocytes in 40 mM Na-borate buffer (pH 7.5) containing 4 mM Mg^{2+}, 0.02% BSA, and 0.75% NaCl at 37°C for 30 min. Hemolytic activity in terms of percent hemolysis, evaluated to measure the A_{550} value of the 500 ×*g* supernatant of the reaction mixture, was plotted as a function of the amount of protein, and the amounts of protein required for 50% hemolysis (HD_{50}) were calculated from the inflection points of the sigmoid curves. (c) Hemolytic activities of the WT (solid square) and E53D (solid circle) mutant SMases were plotted as a function of the concentration of Ca^{2+} and the Ca^{2+} concentrations required for 50% activation were calculated by sigmoid curve fitting.

products, *E. coli* transformants of the resulting recombinant plasmids were used for the following experiments.

To estimate hemolytic activity of Glu-53 mutant enzymes, *E. coli* transformants producing Glu-53 mutant SMases were cultured on agar plates containing 2.5% bovine erythrocytes. As shown in Fig. 2a, the hemolytic activities of the mutant SMases were evaluated by the area size of the hemolytic zones that appeared around the grown *E. coli* cell mass. The hemolytic activity of the E53D mutant was decreased to less than 40% that of the WT enzyme. Moreover, the hemolytic activities of the E53A and E53Q mutant enzymes proved to be completely abolished. Comparable results were obtained for the hydrolytic activities of the crude cell extracts of the *E. coli* transformants using mixed-micellar SM with Triton X-100 as a substrate. Substitution of Glu-53 with Asp reduced the hydrolytic activity to less than 2% (23 ± 1 mU/mg protein) that of the WT enzyme ($1.3 \times 10^3 \pm 0.0$ mU/mg protein), and the E53A and E53Q mutations abolished the activity to the level of the vector control (0.17 ± 0.03 mU/mg protein). These data suggest that the negative charge of the -COO^- of Glu-53 is important for enzymatic catalysis.

Effect of E53D Mutation on Hydrolytic and Hemolytic Activities—To elucidate the effect of the E53D mutation on enzymatic function in detail, the WT and E53D mutant SMases were purified to homogeneity as described in "MATERIALS AND METHODS." The hydrolytic activities of the WT and E53D mutant enzymes were measured not only for SM, a natural substrate, but also for phosphocholine-containing analogs, HNP, Lyso-PC, and *p*-NPPC. These substrates differ in hydrophobicity due to their differing hydrocarbon chains. As shown in Table 1, the E53D mutation caused a substantial reduction in the hydrolytic activity. In SM hydrolysis, this mutation brought about a 21-fold reduction in k_{cat} as compared with that of the WT enzyme. The apparent K_m for SM hydrolysis was slightly increased, and resultingly, the apparent k_{cat}/K_m was significantly decreased by the mutation. When more hydrophilic substrates such as HNP, Lyso-PC, and *p*-NPPC were used, the hydrolytic activities were exhaustively lowered to a level of 10^{-2} to 10^{-4} that of the WT enzyme. These data indicate that Glu-53 is directly involved in catalysis rather than in substrate binding.

The hemolytic activity of the E53D mutant enzyme was measured in the presence of 4 mM Mg^{2+} (Fig. 2 b). The amount of protein required for 50% hemolysis (HD_{50}) was increased to 150-fold that of the WT enzyme by the mutation. Time course analysis of hemolytic activity showed that the hemolytic action of the E53D mutant proceeds more slowly than that of the WT enzyme (data not shown), indicating that the specific activity of the E53D mutant enzyme for hemolysis is remarkably decreased.

We previously demonstrated that the hemolytic activity of *B. cereus* SMase is activated in the coexistence of Ca^{2+} and Mg^{2+} (*7*, *19–21*). Ca^{2+} accelerates adsorption of the enzyme protein to the erythrocyte membrane. Our recent study showed that Asp-100 acts as a ligand for Ca^{2+} binding (Obama, T., Ikezawa, H., Imagawa, M., and Tsukamoto, K., to be published elsewhere). The structural model suggests that Glu-53 must be located in the

Table 1. **Kinetic parameters of the purified WT and mutant SMases for hydrolysis of SM and other phosphocholine-containing substrates.**

	$k_{cat} \times 10^{-2}$ (min^{-1})				K_m (mM)	$k_{cat} \times 10^{-2}/K_m$ (min^{-1}·mM^{-1})
SMase	SM	HNP	Lyso-PC	*p*-NPPC	SM	SM
WT	210 ± 10	5.9 ± 0.2	13 ± 0	$9.2 \times 10^{-2} \pm 0.1 \times 10^{-2}$	0.35 ± 0.03	600
E53D	10 ± 0	$9.5 \times 10^{-4} \pm 1.2 \times 10^{-4}$	$3.5 \times 10^{-3} \pm 0.4 \times 10^{-3}$	$2.6 \times 10^{-4} \pm 0.1 \times 10^{-4}$	2.0 ± 0.1	5.0

vicinity of Asp-100 (*12*). To test the possibility that Glu-53 is a ligand for Ca^{2+}, the effect of E53D mutation on the Ca^{2+}-dependent activation of hemolysis was examined. The E53D enzyme partially retained hemolytic activity but the hemolysis proceeded more slowly compared with the WT enzyme. However, hemolysis induced by the E53D enzyme reached a plateau at the same level as the WT (data not shown). Furthermore, the Ca^{2+} concentration required for 50% hemolysis by the E53D enzyme was almost the same as that of the WT enzyme (Fig. 2c). In fact, the Ca^{2+}-dependent activation of hemolysis by the E53D enzyme was quite similar to that by the WT enzyme. These data indicate that the amount of E53D mutant enzyme bound to erythrocyte membrane is almost the same degree as that of the WT enzyme during hemolysis. The results clearly rule out the possibility that Glu-53 acts as a ligand for Ca^{2+}. Therefore, the decrease in hemolytic activity by the E53D mutation may be attributed to a reduction in catalytic efficiency.

Effect of E53D Mutation on Mg^{2+} Dependency in SM Hydrolysis—Mg^{2+} is an essential component of SMase for catalytic activity (*18*). To examine the effect of the E53D mutation on the Mg^{2+} dependency for catalysis, the SM-hydrolyzing activities of the WT and E53D mutant enzymes were measured at various concentrations of Mg^{2+}. As shown in Fig. 3, the effect of Mg^{2+} on the WT enzyme is characterized by a two-step activation. Under physiological conditions, the high-affinity Mg^{2+}-binding site (50% saturation at 4.1 μM) would be saturated when the activity reaches almost 80% of the full activity. For additional activation, saturation of the low-affinity binding site (50% saturation at 20 mM) should be required. These data suggest that at least two binding sites for Mg^{2+} are present on the WT enzyme. By E53D mutation, the high-affinity binding site shifts to the right (0.23 mM) in the activation curve, resulting in an apparent one-step activation under the experimental conditions. It is supposed that the E53D mutation decreases the binding affinity of Mg^{2+} for the high-affinity site. These data strongly suggest that Glu-53 is involved in the high-affinity binding site for Mg^{2+}, acting as a ligand for Mg^{2+}. We considered the possibility that the low-affinity binding site might shift rightward by the mutation, however, we could not confirm the presence of a second activation at high concentrations (>300 mM) of Mg^{2+} due to aggregation of the SM-micelles.

To hold the Mg^{2+} ion in an appropriate position for catalytic action of the enzyme, another Mg^{2+} ligand must exist. The 3D model indicates that the conserved His-151 is supposed to act as an acid in enzyme catalysis and is located in the vicinity of Glu-53. To examine whether His-151 could act as another ligand for Mg^{2+}, the Mg^{2+} dependency of SM hydrolysis was measured using the H151A mutant enzyme whose SM-hydrolyzing activity is decreased to a level 3×10^{-3} that of the WT enzyme. The Mg^{2+} concentration required for 50% saturation of the high-affinity site was not affected (data not shown), suggesting that His-151 is not a ligand for Mg^{2+}.

Effect of E53D Mutation on the Action of Activating and Inhibitory Divalent Cations—It is known that Mn^{2+} and Co^{2+} partially compensate for the function of essential Mg^{2+}, and activate the SM-hydrolyzing activity of the WT enzyme (*7*). Mg^{2+} in the high-affinity site can be replaced by 0.87 μM Mn^{2+} or 1.5 μM Co^{2+} where 50% activation of SMase is exhibited (Fig. 4, a and b). If Glu-53 acts as a ligand for Mg^{2+}, E53D mutation should affect the optimal conditions for activation by these divalent cations. To verify this hypothesis, the effect of E53D mutation on Mn^{2+}- and Co^{2+}-dependent activation

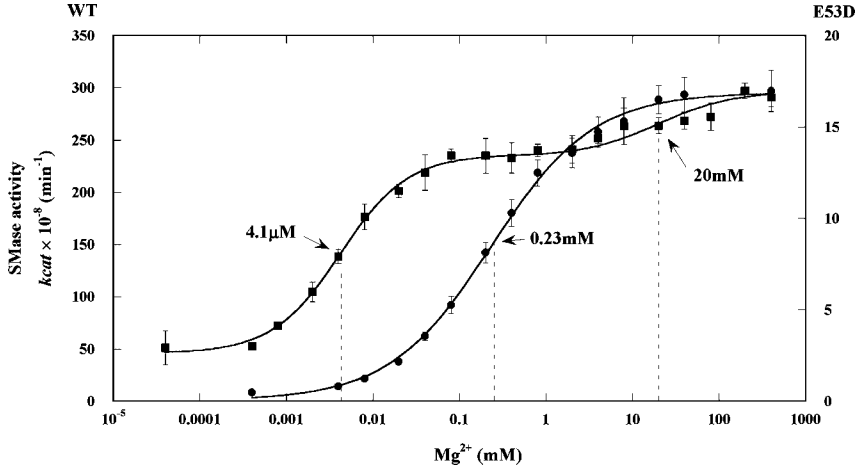

Fig. 3. **Mg^{2+}-dependent activation of the WT and E53D mutant SMases.** The SM-hydrolyzing activities of the WT (solid square) and E53D (solid circle) mutant enzymes were measured in 40 mM Na-borate buffer (pH 7.5) containing 2 mM SM, 0.312% Triton X-100 and varying concentrations of $MgCl_2$. The reaction was stopped by the addition of $CHCl_3$/MeOH/HCl (66:33:1) and immediate vortex mixing, followed by centrifugation at 2,000 ×*g* for 2 min. The resulting phosphocholine in the aqueous layer was estimated as the SM-hydrolyzing activity. All data were fitted to a sigmoid curve to estimate the 50% effective concentration. The curve for the WT enzyme was drawn as a combination of sigmoid curves separately analyzed for the high- (up to 0.4 mM of Mg^{2+}) and low- (0.4 to 300 mM of Mg^{2+}) affinity Mg^{2+} binding sites.

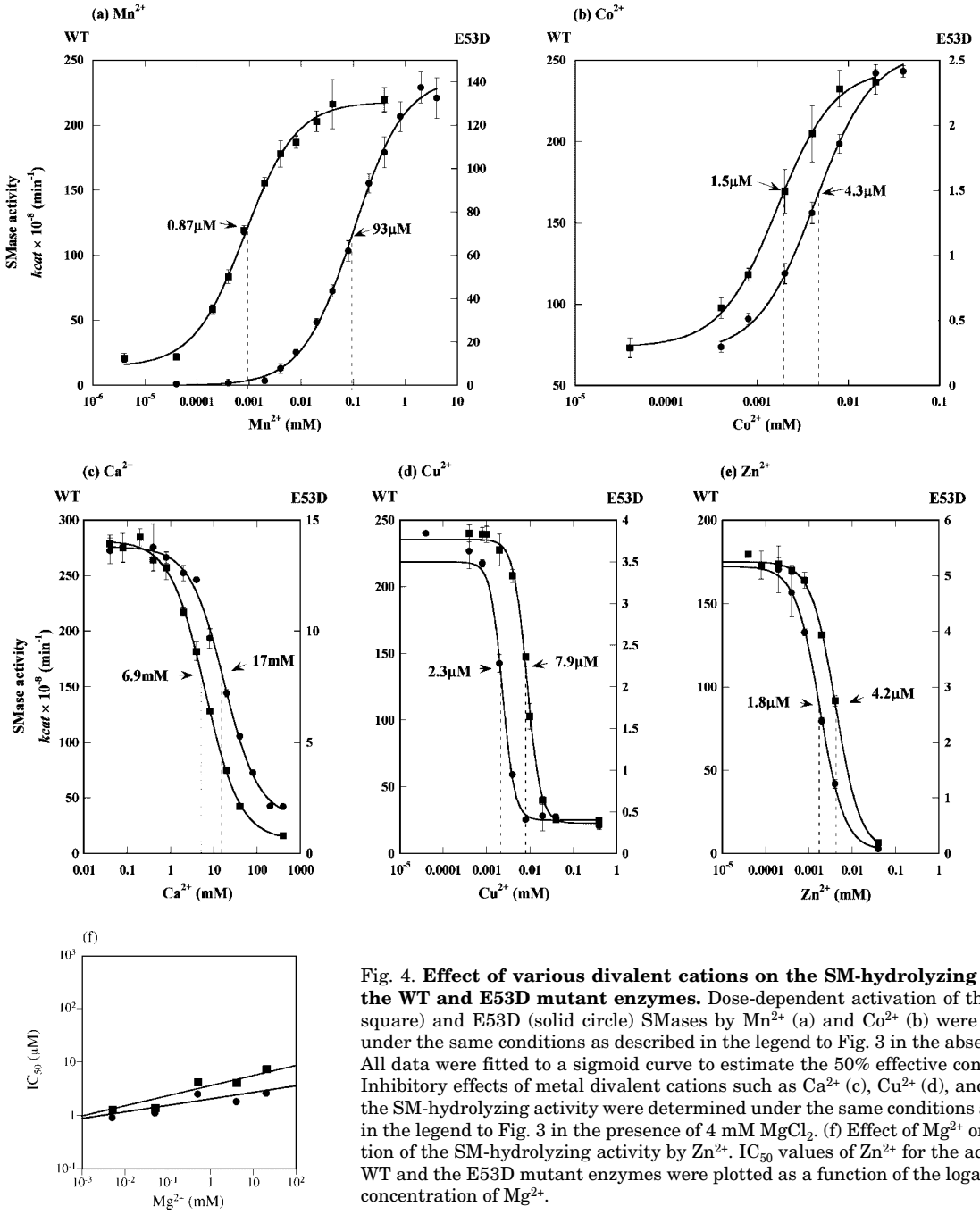

Fig. 4. **Effect of various divalent cations on the SM-hydrolyzing activity of the WT and E53D mutant enzymes.** Dose-dependent activation of the WT (solid square) and E53D (solid circle) SMases by Mn^{2+} (a) and Co^{2+} (b) were determined under the same conditions as described in the legend to Fig. 3 in the absence of Mg^{2+}. All data were fitted to a sigmoid curve to estimate the 50% effective concentrations. Inhibitory effects of metal divalent cations such as Ca^{2+} (c), Cu^{2+} (d), and Zn^{2+} (e) on the SM-hydrolyzing activity were determined under the same conditions as described in the legend to Fig. 3 in the presence of 4 mM $MgCl_2$. (f) Effect of Mg^{2+} on the inhibition of the SM-hydrolyzing activity by Zn^{2+}. IC_{50} values of Zn^{2+} for the activity of the WT and the E53D mutant enzymes were plotted as a function of the logarithm of the concentration of Mg^{2+}.

was measured for SM hydrolysis in the absence of Mg^{2+}. The concentration of Mn^{2+} and Co^{2+} required for 50% activation was elevated by the E53D mutation to 100- and 3-fold higher than that of the WT enzyme, respectively (Fig. 4, a and b). The observation is consistent with the effect of this mutation on Mg^{2+} sensitivity. By E53D mutation, the enzyme affinities for Mn^{2+} and Co^{2+} were reduced. Mn^{2+} and Co^{2+} are assumed to bind to the same high-affinity site as Mg^{2+}.

We previously found that divalent cations such as Ca^{2+}, Zn^{2+}, and Cu^{2+} inhibit the catalytic activity of *B. cereus* SMase (7), however, a detailed mechanism of their inhibitory effects remains unclarified. To investigate the mechanism of inhibition and the relationship between the inhibitory effect and the Mg^{2+}-binding sites, the SM-hydrolyzing activity of the E53D mutant enzyme was measured in the presence of these inhibitory divalent cations with 4 mM Mg^{2+}. The E53D mutation induced a slight shift in the IC_{50} values of Ca^{2+}, Cu^{2+}, and Zn^{2+} from 6.9 mM to 17 mM, 7.9 μM to 2.3 μM, and 4.2 μM to 1.8 μM, respectively. Therefore, the inhibitory effects of these cations are not affected very much by this mutation (Fig. 4, c, d, and e). As an example of these cations, the IC_{50} of Zn^{2+} for SM hydrolysis was measured in the presence of Mg^{2+} at concentrations varying from 4 μM to 20 mM (Fig. 4f). This range of Mg^{2+} concentration fully covers the con-

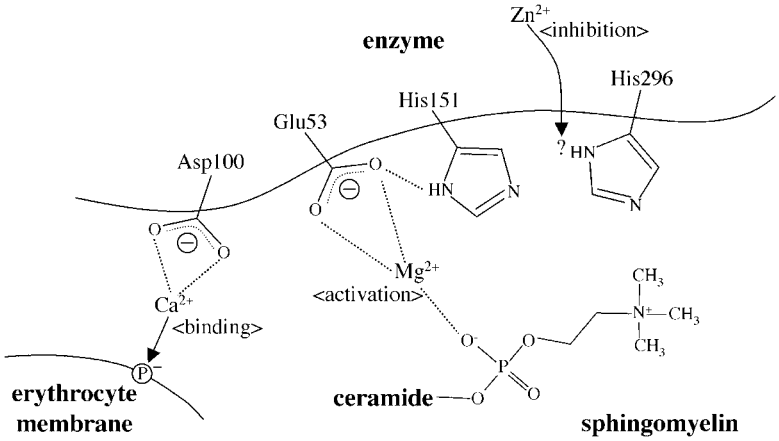

Fig. 5. **Metal-binding sites of SMase.** The residues playing important roles as ligands for Ca^{2+}, required for adsorption onto the erythrocyte membrane, and Mg^{2+}, indispensable for activation of the hydrolytic activity of the enzyme, are indicated. Glu-53 acts as a ligand for Mg^{2+}, which coordinates with a phosphate group on the substrate. Inhibitory divalent cations, such as Zn^{2+}, are supposed to act at a site different from that of Mg^{2+}

centrations saturating not only the high- but also the low-affinity Mg^{2+} binding sites. The IC_{50} of Zn^{2+} for the WT enzyme increased with Mg^{2+} concentration, indicating that higher concentrations of Mg^{2+} slightly restore the inhibition caused by Zn^{2+}. In the E53D mutant enzyme, the inhibitory effect of Zn^{2+} was also reversed by high concentrations of Mg^{2+}, but not so significantly. These results show that the E53D mutation does not alter the sensitivity of the enzyme to inhibition by these cations.

We further analyzed whether Zn^{2+} can bind to the enzyme or not. By atomic absorption spectrometry, 1.13 ± 0.03 mol of Zn^{2+} proved to be bound to 1 mol of WT SMase protein. The amount of Zn^{2+} bound to the E53D SMase protein was not affected by the mutation (1.08 ± 0.06 per 1 mol enzyme protein), suggesting that Glu-53 is not a ligand for Zn^{2+}. His is well known as a good ligand for Zn^{2+}. To examine whether His-151 can act as a ligand for Zn^{2+}, the amount of Zn^{2+} bound to the H151A mutant protein was measured. Equimolar Zn^{2+}-binding to the H151A mutant protein (0.93 ± 0.02 per 1 mol protein) was also observed, indicating that His-151 is not a ligand for Zn^{2+}.

DISCUSSION

In this report, we investigated the function of Glu-53 in *B. cereus* SMase catalysis. Glu-53 is evolutionarily conserved among Mg^{2+}-dependent nSMases from bacteria to mammals. The 3D model of *B. cereus* SMase shows that Glu-53 is located in the vicinity of two histidine residues (His-151 and His-296) essential for catalysis of the enzyme, suggesting that Glu-53 is important for its catalytic function (*12*). Alignment of the amino acid sequences of Mg^{2+}-dependent nSMases with that of bovine pancreatic DNase I, which has structural compatibility with *B. cereus* SMase, shows that the conserved Glu-53 corresponds to Glu-39 in DNase I (*12*, *22*, *23*). Crystallographic analysis of DNase I associated with double-stranded oligonucleotide provides insight into its catalytic mechanism as a general acid-base catalyst (*24*). As in the case of His-151 and His-296 of *B. cereus* SMase (*12*), an enzymatic assay based on site-directed mutagenesis reveals the importance of catalytic residues such as His-134 and His-252 in this DNase molecule, in which they are supposed to function as a general acid and a general base, respectively. Although Glu-39 is assumed to play a role in Mg^{2+}-binding based on crystallographic studies, a detailed enzymatic analysis of Glu-39 as a ligand for catalytically essential Mg^{2+} was not achieved.

In this study, we constructed Glu-53-substituted mutant enzymes, E53A, E53Q, and E53D. Among them, only the E53D mutant enzyme partially retained its hemolytic and hydrolytic activities. A structurally conserved mutation (E53Q) could not compensate for the function of Glu-53. This is consistent with the observation that the transient expression of SMase activity in HEK293 cells transfected with the human nSMase 1 cDNA is abolished by E49Q mutation (*25*). These data suggest that the negative carboxyl charge of Glu-53 is indispensable for its enzymatic function. Analyses of hydrolytic and hemolytic activities of the purified WT

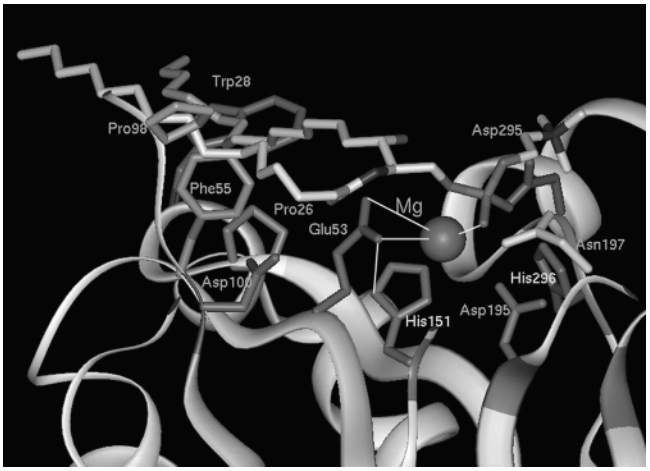

Fig. 6. **3D model of the SMase-Mg^{2+}-SM complex.** The disposition of SM was speculated not only by fitting a phosphate group into the essential catalytic residues, but also by considering the interaction between the hydrocarbon chains of the substrate and a series of hydrophobic residues on the surface of the enzyme. His-151 and His-296 provide general acid and general base catalysis, respectively. A Mg^{2+} ion stabilizes the penta-covalent intermediate and facilitates the attack of hydroxide ion through co-ordination with Glu-53 and the non-bridging oxygen atom of the scissile phosphate.

and E53D mutant enzymes clearly demonstrate that Glu-53 is a critical residue for enzyme catalysis as a ligand for essential Mg^{2+}. In eukaryotic nSMases, a corresponding residue, such as Glu49 in human nSMase 1, must play a similar role in catalytic function. Site-directed mutagenesis of human apurinic/apyrimidinic endonuclease 1 (HAP1) (*26*, *27*), which has a fold and catalytically similar structure to that of DNase I as well as exonuclease I (EXO III) (*28*), provides evidence of the importance of Glu-96 in catalytically essential Mg^{2+}-binding as in the case of Glu-53 in *B. cereus* SMase. The E96A mutant exhibits 400-fold reduced catalytic activity and requires abnormally high amounts of exogenous divalent metal ions for activity.

Analysis of the Mg^{2+} dependency of enzymatic catalysis showed that Mg^{2+} activation of *B. cereus* SMase is critical at two distinct concentrations, indicating the existence of at least two different Mg^{2+} binding sites, high- and low-affinity sites. This is consistent with the previous observation of a change in the tryptophanyl fluorescence intensity by Mg^{2+} binding to the enzyme (*29*). The E53D mutation was supposed to affect the high-affinity binding site and result in a one-step activation by Mg^{2+}, suggesting Glu-53 is involved in the high-affinity binding site of Mg^{2+}. This observation was further confirmed by examining the effect of the E53D mutation on the activation of SM hydrolysis by Mn^{2+} and Co^{2+} instead of Mg^{2+}. The mutation causes a reduction in the affinities of these compensating cations for catalytic activation of the enzyme.

In contrast, the inhibitory actions of Ca^{2+}, $Cu^{2+,}$ and Zn^{2+} for catalysis were not influenced by the E53D mutation. If Zn^{2+} competes with Mg^{2+} at its binding sites on the enzyme, it would be expected that the E53D mutation would induce a change in the inhibitory effect of Zn^{2+}. However, the IC_{50} of Zn^{2+} for SM hydrolysis was almost the same as that of the WT enzyme in the presence of various concentrations of Mg^{2+}. Moreover, equimolar binding of Zn^{2+} to both of the WT and E53D proteins was observed. These data indicate that the binding site of Zn^{2+} differs from that of the catalytically essential Mg^{2+}. Also, the results are consistent with our previous finding that Zn^{2+} inhibition is not competitive with Mg^{2+} (*7*). The 3D model of the enzyme implies that His-151 might play a role as another ligand for Mg^{2+}, or inhibitory Zn^{2+}. But the Mg^{2+} dependency of the catalytic action of the H151A mutant enzyme was the same as that of the WT enzyme, and the H151A mutation did not affect the amount of Zn^{2+} bound to the enzyme protein. These data demonstrate that His-151 is not a ligand for Mg^{2+} or Zn^{2+}.

We failed to detect appreciable Mg^{2+} binding to the enzyme protein by atomic absorption spectroscopy. This is consistent with the experiment that examined the stability of the metal ion bound to the recombinant HAP1 protein by atomic absorption spectrometry (*26*). It is generally considered that Mg^{2+} may be introduced into the active site pocket of the enzyme together with the phosphate backbone of a substrate molecule, for example, yeast phosphoglycerate kinase (*30*). On the basis of the crystal structures of DNase I, HAP1, and EXO III, the metal ion is supposed to be required to stabilize the catalytic intermediate and facilitate the attack on the phosphodiester backbone of the activated hydroxide ion. We previously showed the existence of a high-affinity Mg^{2+} binding site on the enzyme with a very small dissociation constant by the equilibrium dialysis method (*29*). This suggests the requirement of a phosphate group on the substrate for Mg^{2+} binding. Appropriate substrate analogues stable to hydrolysis should be designed and synthesized to prove this hypothesis. On the basis of this study and the predicted 3D structure of *B. cereus* SMase, Fig. 5 shows a schematic diagram of the divalent cation binding sites important for enzymatic function. Mg^{2+}, indispensable for catalysis, is shown to be associated with Glu-53. This high-affinity Mg^{2+}-binding site must be different from the binding sites of inhibitory metal ions such as Zn^{2+}, $Cu^{2+,}$ and Ca^{2+}. Figure 6 shows a close-up view of the catalytic pocket of *B. cereus* SMase. An appropriate position for the substrate, SM, was estimated in our previous report (*12*). Some hydrophobic residues, such as Trp-28 and Phe-55, are likely to interact with the hydrocarbon chains of SM. In this mode, Glu-53 lies in an appropriate orientation to act as a ligand for Mg^{2+}, suggesting the possibility of coordination among Glu-53, Mg^{2+} and a phosphate group, as well as hydrogen bonding between the carboxylate group of Glu-53 and the imidazole N of His-151. Glu-53 may function not only as a ligand for Mg^{2+}, but also as a support for maintaining His-151 in the correct position to achieve acid-base catalysis. Coordination among Glu-53, His-151, $Mg^{2+,}$ and the phosphate backbone of the substrate promotes an increase in the pK_a value of His-151 and supports the transiently protonated state of His-151 assumed to act as a general acid to provide a proton to the penta-covalent transition intermediate. Mg^{2+} is also supposed to stabilize the penta-covalent intermediate through the network.

REFERENCES

1. Schissel, S.L., Schuchman, E.H., Williams, K.J., and Tabas, I. (1996) Zn^{2+}-stimulated sphingomyelinase is secreted by many cell types and is a product of the acid sphingomyelinase gene. *J. Biol. Chem.* **271**, 18431–18436
2. Okazaki, T., Bielawska, A., Domae, N., Bell, R.M., and Hannun, Y.A. (1994) Characteristics and partial purification of a novel cytosolic, magnesium-independent, neutral sphingomyelinase activated in the early signal transduction of 1 alpha, 25-dihydroxyvitamin D3-induced HL-60 cell differentiation. *J. Biol. Chem.* **269**, 4070–4077
3. Tomiuk, S., Hofmann, K., Nix, M., Zumbansen, M., and Stoffel, W. (1998) Cloned mammalian neutral sphingomyelinase: functions in sphingolipid signaling? *Proc. Natl. Acad. Sci. USA* **95**, 3638–3643
4. Hofmann, K., Tomiuk, S., Wolff, G., and Stoffel, W. (2000) Cloning and characterization of the mammalian brain-specific, Mg^{2+}-dependent neutral sphingomyelinase. *Proc. Natl. Acad. Sci. USA* **97**, 5895–5900
5. Cheng, Y., Nilsson, A., Tomquist, E., and Duan, R.D. (2002) Purification, characterization, and expression of rat intestinal alkaline sphingomyelinase. *J. Lipid Res.* **43**, 316–324
6. Tomita, M., Taguchi, R., and Ikezawa, H. (1991) Sphingomyelinase of *Bacillus cereus* as a bacterial hemolysin. *J. Toxicol.-Toxin Rev.* **10**, 169–207
7. Ikezawa, H., Matsushita, M., Tomita, M., and Taguchi, R. (1986) Effect of metal ions on sphingomyelinase activity of *Bacillus cereus*. *Arch.Biochem.Biophys.* **249**, 588–595
8. Yu, B.Z., Zakim, D., and Jain, M.K. (2002) Processive interfacial catalytic turnover by *Bacillus cereus* sphingomyelinase on sphingomyelin vesicles. *Biochim. Biophys. Acta* **1583**, 122–132

9. Levade, T. and Jaffrezou, J.P. (1999) Signalling sphingomyelinases: which, where, how and why? *Biochim. Biophys. Acta* **1438**, 1–17
10. Hannun, Y.A., Luberto, C., and Argraves, K.M. (2001) Enzyme of sphingolipid metabolism: from modulator to integrative signaling. *Biochemistry* **40**, 4893–4903
11. Tamura, H., Tameishi, K., Yamada, A., Tomita, M., Matsuo, Y., Nishikawa, K., and Ikezawa, H. (1995) Mutation in aspartic acid residues modifies catalytic and hemolytic activities of *Bacillus cereus* sphingomyelinase. *Biochem. J.* **309**, 757–764
12. Matsuo, Y., Yamada, A., Tsukamoto, K., Tamura, H., Ikezawa, H., Nakamura, H., and Nishikawa, K. (1996) A distant evolutionary relationship between bacterial sphingomyelinase and mammalian DNase I. *Protein Sci.* **5**, 2459–2467
13. Spanner, S. (1973) Separation and analysis of phospholipids in *Form and Function of Phospholipids* (Ansell, G.B., Hawthrone, J.N., and Dawson, R.M.C., eds.) pp. 43–65, Elsevier, Amsterdam
14. Bligh, E.G. and Dyer, W.J. (1959) A rapid method of total lipid extraction and purification. *Can. J. Biochem. Physiol.* **37**, 911–917
15. Yamada, A., Tsukagoshi, N., Udaka, S., Sasaki, T., Makino, S., Nakamura, S., Little, C., Tomita, M., and Ikezawa, H. (1988) Nucleotide sequence and expression in *Escherichia coli* of the gene coding for sphingomyelinase of *Bacillus cereus*. *Eur. J. Biochem.* **175**, 213–220
16. Weiner, M.P. and Costa, G.L. (1995) Rapid PCR site-directed mutagenesis in *PCR Primer* (Dieffenbach, C.W. and Dveksler, G.S., ed.) pp. 613–621, Cold Spring Harbor Laboratory Press, Cold Spring Harbor, NY
17. Tamura, H., Tameishi, K., Yamagata, H., Udaka, S., Kobayashi, T., Tomita, M., and Ikezawa, H. (1992) Mass production of sphingomyelinase of *Bacillus cereus* by a protein-hyperproducing strain, *Bacillus brevis* 47, and its purification. *J. Biochem.* **112**, 488–491
18. Tomita, M., Taguchi, R., and Ikezawa, H. (1982) Molecular properties and kinetic studies on sphingomyelinase of *Bacillus cereus*. *Biochim. Biophys. Acta* **704**, 90–99
19. Ikezawa, H., Mori, M., and Taguchi, R. (1980) Studies on sphingomyelinase of *Bacillus cereus*: hydrolytic and hemolytic action on erythrocyte membranes. *Arch. Biochem. Biophys.* **199**, 572–578
20. Tomita, M., Taguchi, R., and Ikezawa, H. (1983) The action of sphingomyelinase of *Bacillus cereus* on bovine erythrocyte membrane and liposomes: specific adsorption onto these membranes. *J. Biochem.* **93**, 1221–1230
21. Tomita, M., Taguchi, R., and Ikezawa, H. (1983) Adsorption of sphingomyelinase of *Bacillus cereus* onto erythrocyte membranes. *Arch. Biochem. Biophys.* **223**, 202–212
22. Suck, D., Lahm, A., and Oefner, C. (1988) Structure refined to 2Å of a nicked DNA octanucleotide complex with DNase I. *Nature* **322**, 464–468
23. Weston, S.A., Lahm, A., and Suck, D. (1992) X-ray structure of the DNase I-d(GGTATACC)$_2$ complex at 2.3 Å resolution. *J. Mol. Biol.* **226**, 1237–1256
24. Stephen, J.J., Andrew, F.W., and Bernard, A.C. (1996) Site-directed mutagenesis of the catalytic residues of bovine pancreatic deoxyribonuclease I. *J. Mol. Biol.* **264**, 1154–1163
25. Tomiuk S., Zumbansen M., and Stoffel W. (2000) Characterization and subcellular localization of murine and human magnesium-dependent neutral sphingomyelinase. *J. Biol. Chem.* **275**, 5710–5717
26. Barzilay, G., Mol, C.D., Robson, C.N., Walker, L.J., Cunningham, R.P., Tainer, J.A., and Hickson, I.D. (1995) Identification of critical active-site residues in the multifunctional human DNA repair enzyme HAP1. *Nat. Struct. Biol.* **2**, 561–568
27. Gorman M.A., Morera, S., Rothwell, D.G., de La Fortelle, E., Mol, C.D., Tainer, J.A., Hickson, I.D., and Freemont, P.S. (1997) The crystal structure of the human DNA repair endonuclease HAP1 suggests the recognition of extra-helical deoxyribose at DNA abasic sites. *EMBO J.* **16**, 6548–6558
28. Mol, C.D., Kuo, C.F., Thayer, M.M., Cunningham, R.P., and Tainer, J.A., (1995) Structure and function of the multifunctional DNA-repair enzyme exonuclease III. *Nature* **374**, 381–386
29. Fujii, S., Inoue, B., Yamamoto, H., Ogata, K., Shinki, T., Inoue, S., Tomita, M., Tamura, H., Tsukamoto, K., Ikezawa, H., and Ikeda, K. (1998) Mg^{2+} binding and catalytic function of sphingomyelinase from *Bacillus cereus*. *J. Biochem.* **124**, 1178–1187
30. Watson, H.C., Walker, N.P.C., Shaw, P.J., Bryant, T.N., Wendell, P.L., Fothergill, L.A., Perkins, R.E., Conroy, S.C., Dobson, M.J., Tuite, M.F., Kingsman, A.J., and Kingsman, S.M. (1982) Sequence and structure of yeast phosphoglycerate kinase. *EMBO J.* **1**, 1635–1640